Asymptotic Scaling Behavior of Self-Avoiding Walks on Critical Percolation Clusters

Niklas Fricke[*] and Wolfhard Janke[†]

Institut für Theoretische Physik and Centre for Theoretical Sciences (NTZ), Universität Leipzig,
Postfach 100920, D-04009 Leipzig, Germany

We study self-avoiding walks on three-dimensional critical percolation clusters using a new exact enumeration method. It overcomes the exponential increase in computation time by exploiting the clusters' fractal nature. We enumerate walks of over 10^4 steps, far more than has ever been possible. The scaling exponent ν for the end-to-end distance turns out to be smaller than previously thought and appears to be the same on the backbones as on full clusters. We find strong evidence against the widely assumed scaling law for the number of conformations and propose an alternative, which perfectly fits our data.

The self-avoiding walk (SAW) [1] is a fundamental model in statistical mechanics and crucial for our understanding of the scaling behavior of polymers [2]. Asymptotically, it is characterized by universal exponents, which are related to the critical exponents of spin systems and assumed to describe long, flexible polymers in good solvent condition. While much is known about SAWs on regular lattices, their behavior in disordered environments, such as porous rocks or biological cells, is less understood. The paradigmatic model for such systems are SAWs on critical percolation clusters [3,4]. Here the walks can only visit a random fraction of sites, whose concentration is equal to the percolation threshold of the lattice. This critical concentration may not be realistic, but it represents an important limiting case, and the effect of the critical clusters' fractal structure is particularly intriguing [5].

One usually considers quenched disorder averages, here denoted by square brackets: On each disorder realization ("cluster"), one takes the average over all walk conformations of length N. Each such conformational average contributes equally to the disorder average. It is assumed that the average number of conformations $[Z]$ and their mean squared end-to-end distance $[\langle R^2 \rangle]$ follow asymptotic scaling laws similar to those for normal SAWs:

$$[Z] \sim \mu^N N^{\gamma - 1}, \tag{1}$$

$$[\langle R^2 \rangle] \sim N^{2\nu} = N^{2/d_f}. \tag{2}$$

γ and ν are universal scaling exponents, d_f is the SAW's fractal (Hausdorff) dimension, and μ is a lattice-dependent effective connectivity constant. While the effect of the fractal disorder on γ and μ is still very controversial, there is convincing evidence that ν is different than on regular lattices [6]. However, there is uncertainty concerning the actual value despite a considerable amount of work dedicated to the system. Analytical works, employing real-space and field-theoretical renormalization group

methods, have yielded conflicting results [6–12], while accuracy and reliability of numerical investigations have been poor due to modest system and sample sizes. In most numerical studies (see for instance [13–17]), exact enumeration was used to determine the conformational averages. Owing to exponentially increasing computation time [see Eq. (1)], the length of the walks was restricted to 30–50. Chain-growth Monte Carlo methods may allow for more than a hundred steps [18–22], but they add statistical uncertainty and the danger of biased results [23].

We recently developed a new algorithm for exact enumeration of SAWs on two-dimensional critical percolation clusters [24], which we have now generalized to higher dimensions. By making use of the clusters' fractal properties, it overcomes the exponential increase in computation time that usually affects exact enumeration methods. Walks of over 10^4 steps are now accessible, permitting a much more refined investigation of the system. Indeed, we think that the true asymptotic behavior may now be revealed for the first time.

Our method exploits the self-similar nature of the clusters to factorize the counting problem hierarchically, drawing on the ideas of renormalization group theory. The key lies in the observation that the connectivity of a critical percolation cluster is extremely low on any length scale. This is best appreciated by looking at the backbone of a cluster (Fig. 1), the part that remains when all singly connected "dangling ends" are removed. We define it as the largest biconnected component, i.e., the largest piece from which nothing can be disconnected by removing a single site. The fragile structure of the backbone, which is the most connected part, suggests that the whole cluster can be decomposed into separate regions by removing only a small number of sites [25]. This applies on all length scales, so that we can organize the cluster into a hierarchy of nested "blobs" as sketched in Fig. 2. Each blob should have very few $[\approx O(1)]$ external connections and should not contain too much mass (colored areas in Fig. 2) that is
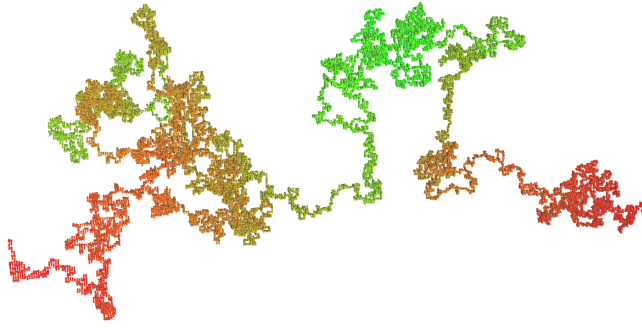
FIG. 1 (color online). Backbone of a critical percolation cluster on a cubic lattice of 300^3 sites. The two ends are connected via periodic boundary conditions; coloring indicates shortest-path distance to the origin.

not encapsulated in smaller blobs. We create the blob hierarchy by repeatedly fusing regions with many interconnections, aiming for an optimal balance between the two requirements.

The principle idea now is to factorize the enumeration procedure by treating walk segments through different blobs separately. The self-similarity of the system suggests a "renormalization" approach: We start by enumerating all walk conformations within smallest blobs ("children") that are contained within larger ones ("parents"). We use the standard backtracking routine [13–17] for this but distinguish different classes of paths depending on the external connections they are linked to. When we later generate the paths through the parents, the children are treated as single sites, but we note by which links they are accessed and left. This information is needed to properly match the paths to the segments through the children once the counting within the parents is done. Now we can delete all information concerning the children and proceed on to the "grandparents." This can be regarded as an exact renormalization procedure with adaptive cells (blobs): Internal degrees of freedom are "integrated out" (enumerated) and cells decimated to pointlike sites. It is
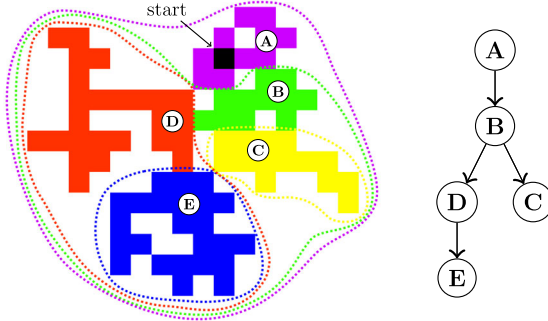

FIG. 2 (color online). Schematic picture of a tree hierarchy of nested blobs. The starting position for the walks is marked black. Walk segments through the blobs are generated in the order $E \rightarrow A$.

repeated up to the largest blob—the region accessible within the maximum number of SAW steps.

These main ideas are simple, but defining the blob hierarchy and matching the path segments is technically challenging. The gain, however, is significant: On a present-day 3 GHz processor, the number of conformations for a 10^4-step SAW (typically 10^{1200}) and their mean end-to-end distance are determined in about ten minutes on average using our current implementation. The exponential complexity has vanished, and we empirically find a polynomial time increase with an exponent around 2.4.

While the method works in any dimension, we here focus on the physically most relevant case of $D = 3$. To generate the clusters, we used a depth-first growth algorithm known as the Leath method [26]. We only consider clusters that percolate according to the "wrapping" criterion [27,28]. The backbones were identified using Tarjan's algorithm [29]. To avoid correlations, independent sets of clusters were used for walks of different lengths, which we increased by factors of $\sqrt{2}$ from $N = 25$ to $N = 12\,800$. Thanks to the method's efficiency, we could afford samples of at least 5×10^4 clusters for each length.

The average squared end-to-end distance as a function of N is shown in Fig. 3 on a double-logarithmic scale. To enhance visibility, the values are divided by $N^{1.33}$, which is close to $N^{2\nu}$ according to previous studies. The curves appear straight initially, but around $N \approx 150$ they notably start to slump, crossing over to a slightly different slope. We hence have to use a lower cutoff, $N_{\min}$, when estimating ν via a least-squares fit of Eq. (2). On the whole ("incipient") clusters (ic), the χ^2 value of the fit becomes close to 1 ($\chi^2 = 1.3$) if we choose $N_{\min} = 800$. This yields a value of
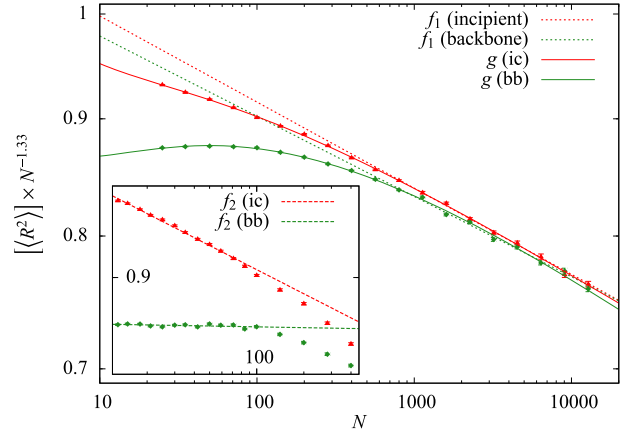

FIG. 3 (color online). Mean squared end-to-end distance vs number of steps for SAWs on incipient critical clusters (red) and backbones (green) on a log-log scale. The lines show the results from different least-squares fits. f_1: Eq. (2) with $N = 800$–$12\,800$ (ic) and $N = 1131$–$12\,800$ (bb); f_2 (inset): Eq. (2), $N = 13$–100; g: Eq. (3), $N = 25$–$12\,800$. The factor $N^{-1.33}$ ($\approx N^{-2\nu}$) serves to magnify the differences.

$\nu_{\text{ic}} = 0.6433(4)$. The fit is shown as dotted red line f_1 in Fig. 3. For the backbones (bb), we get a decent fit ($\chi^2 = 3.4$) with $N_{\min} = 1131$ (dotted green line), which yields a similar result: $\nu_{\text{bb}} = 0.643(1)$. Note that the values of χ^2 are meaningful since the data points are uncorrelated and the errors are purely statistical.

It has often been claimed [16,30–32] that the asymptotic statistics are determined by the backbone alone as a dangling end can only support finite SAWs. As noted in Ref. [19], this argument is questionable since dangling ends come in all sizes and have a larger fractal dimension than the backbone. Still, our results provide strong evidence that $\nu_{\text{ic}} = \nu_{\text{bb}}$ is indeed correct. As demonstrated in Fig. 3, this becomes manifest only for sufficiently long walks. The initial slope on the backbone is slightly larger, and the rate of convergence is lower. This is somewhat surprising: If the effects of the dangling ends vanish with N, it should be the other way around, unless they happen to cancel out other finite-size effects.

The fact that ν_{bb} appears larger initially explains why results for ν from the most recent numerical studies, which only considered the backbones, are significantly larger than ours [0.662(6) [16], 0.667(3) [22]]. The discrepancy is clearly due to the limited system sizes that had been accessible (30 and 80 steps, respectively). To verify this claim, we used an upper cutoff of $N_{\max} = 84$. Since calculations in this regime are swift, we afforded a few more data points and increased the sample sizes to 5×10^5. As can be seen in the inset of Fig. 3, a simple power law nicely fits this data ($\chi^2_{\text{bb}} = 2.0$, $\chi^2_{\text{ic}} = 2.6$); one could hardly suspect a different asymptotic behavior from this perspective. The resulting backbone exponent $\nu_{\text{bb}} = 0.6646(2)$ is consistent with previous findings, though $\nu_{\text{ic}} = 0.6547(2)$ is slightly (but significantly) smaller.

Some of the finite-size effects may be explained by higher-order corrections to Eq. (2). Better fit results over a larger range can indeed be obtained by including the next-to-leading confluent correction term, $N^{2\nu-\Delta}$. In practice, we fit

$$[\langle R^2 \rangle] = a(N + \delta N)^{2\nu}[1 + b/(N + \delta N)^{\Delta}] \qquad (3)$$

as was done for the full-lattice SAW in Ref. [33]. The small shift, which we set to $\delta N = 1/2$, provides for a smoother convergence of the fit but has little effect on the actual results. From the range $N = 25$–$12\,800$ we thus obtain $a_{\text{ic}} = 1.13(2)$, $b_{\text{ic}} = -0.44(3)$, $a_{\text{bb}} = 1.25(5)$, $b_{\text{bb}} = -0.60(1)$, and

$$\nu_{\text{ic}} = 0.644(2), \qquad \Delta_{\text{ic}} = 0.51(5), \qquad (4)$$

$$\nu_{\text{bb}} = 0.640(3), \qquad \Delta_{\text{bb}} = 0.34(4) \qquad (5)$$

as our final estimates [for comparison, $\nu_{\text{full}} = 0.587597(7)$ and $\Delta_{\text{full}} = 0.528(12)$ were found for the regular

simple-cubic lattice [33]]. The fits are shown as continuous curves g in Fig. 3. The χ^2 values are 1.2 (incipient clusters) and 1.6 (backbones). These estimates for ν are consistent with those from the simple fits and again support $\nu_{\text{ic}} = \nu_{\text{bb}}$. We also obtained similar (but less precise) estimates by extrapolating the successive slopes, as was done in [15,16,18]. In terms of the fractal dimensions, $d_f = 1/\nu$, the results are $d_{f,\text{ic}} = 1.553(5)$ and $d_{f,\text{bb}} = 1.563(7)$.

We now turn to the number of conformations, Z. Here we only discuss the results for the incipient clusters; those for the backbones are qualitatively the same. The distribution of Z resembles a lognormal as can be seen in Fig. 4 where we have plotted the measured frequencies of $\ln Z$ for various N alongside normal distributions with the same mean and variance. As noted before [20], such a "multifractal" distribution can be explained by the fact that Z is roughly a product of random variables, namely, the average coordination numbers at each step. Indeed, we find for the variance of $\ln Z$,

$$\sigma^2_{\ln Z} \sim AN^{2\chi}; \quad A = 0.1667(3), \quad \chi = 0.500(1), \qquad (6)$$

which supports this picture. A similar result [$\chi = 0.49(1)$] had been reported previously [15], but there appears yet to be no theoretical explanation why $\chi = 1/2$ should hold exactly.

These large deviations make it hard to obtain unbiased estimates for $[Z]$: The value is easily underestimated if the sample size is too small. We managed to obtain reliable data for $N \leq 200$ by pushing the number of analyzed clusters to 10^7. According to Eq. (1), μ and γ can be estimated by fitting

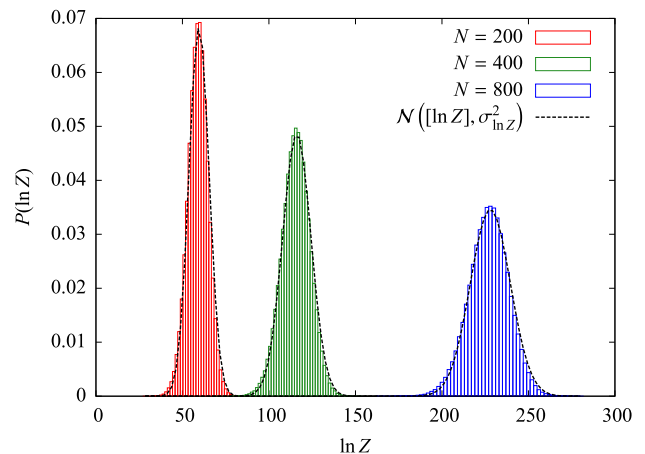$$\ln[Z]/N = \ln a/N + \ln \mu + (\gamma - 1) \ln N/N \qquad (7)$$

FIG. 4 (color online). Measured probability densities of the entropy $\ln Z$ for various lengths. The dashed lines are normal distributions with the same mean values and variances (no fit involved).

as was done in [16,32]. Trying this for different ranges
within $N \le 200$, we found that the estimates for μ (γ)
systematically decrease (increase) with the upper cutoff
N_{max}. This suggests that the asymptotic behavior is not
reached (which would not be surprising given our expe-
rience with ν). From our observations one might hence only
infer the following bounds:

$$\mu < 1.440(4), \qquad \gamma > 1.9(1), \qquad (8)$$

obtained from a fit over $N = 25$–200. However, such a
large value for γ is very different from previous results (see,
e.g., Table 4 in Ref. [32]) and would be highly unusual.

For longer chains, we can only approximate $[Z]$ by
assuming the distribution of Z to be lognormal:

$$[Z] \approx e^{[\ln Z] + \sigma_{\ln Z}^2 / 2} =: [Z_{logn}]. \qquad (9)$$

$[Z_{logn}]$ can be estimated more easily since the "entropies,"
$\ln Z$, are better behaved. In Fig. 5 we have plotted $[\ln Z]/N$,
$\ln[Z]/N$, and $\ln[Z_{logn}]/N$ vs N. As can be seen, $[Z] \approx$
$[Z_{logn}]$ is fulfilled well for small N. For larger N, $\ln[Z]$
appears to approach $[\ln Z]$, which is a consequence of the
aforementioned bias.

The exponential of the mean entropy, $[Z_0] := e^{[\ln Z]}$, is
supposed to follow a scaling law similar to Eq. (1) [16].
Here we have reliable data up to $N = 12\,800$, which
should, in principle, allow for accurate estimates of the
"zeroth moments," μ_0 and γ_0. However, a fit analogous to
Eq. (7) for $[\ln Z]/N$ yields poor results, which remain
strongly dependent on the fit range. (We made a similar
observation for the two-dimensional case [24].) The data
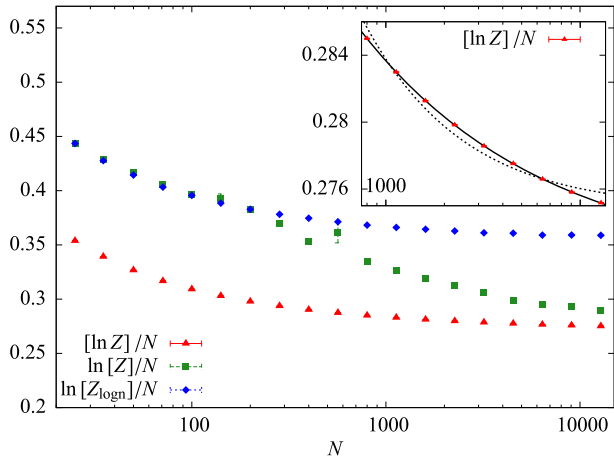are much better described by a function of the form

FIG. 5 (color online).   Mean entropy (red triangles), logarithm
of the average number of conformations (green squares), and
lognormal approximation (blue diamonds) vs N on a log-linear
scale. The estimates for $\ln[Z]$ are biased for $N > 200$ due to large
deviations. The inset shows fits of $[\ln Z]$ using Eq. (7) (dotted)
and Eq. (10) (continuous), respectively.

$$[\ln Z]/N = \ln a/N + (\ln \mu_0)(1 + bN^{-\zeta}) \qquad (10)$$

as can be seen in the inset of Fig. 5. Using Eq. (10), the fit
results stabilize around $N_{min} \approx 800$, which is consistent
with the findings for ν. From the range $N = 800$–$12\,800$ we
obtain $a = 0.7(4)$, $\ln \mu_0 = 0.2715(3)$, $\zeta = 0.48(3)$, and
$b = 1.3(3)$ with $\chi^2 = 0.52$. This would imply

$$[Z_0] \sim \mu_0^{N(1+b/N^\zeta)} \quad \text{with} \quad \mu_0 = 1.3119(3), \qquad (11)$$

rather than a scaling law of the form of Eq. (1). There might
still be a factor $N^{\gamma_0 - 1}$, but we found no numerical evidence
for it. Unfortunately, we cannot do a similar fit for $\ln[Z]/N$
for lack of reliable data points. However, if Eq. (11) is
correct for $[Z_0]$ and assuming Eq. (6), we can infer a similar
law for $[Z_{logn}]$ with $\mu_{logn} = e^{\ln \mu_0 + A/2} = 1.4260(6)$. $[Z] \approx$
$[Z_{logn}]$ would then suggest a scaling law like Eq. (10) for $[Z]$
as well. That approximation is not well founded, so Eq. (1)
might still be correct, but we think that the empirical
evidence against it is significant. In fact, there is also little
theoretical foundation for Eq. (1) other than the analogy to
the regular-lattice case where numerical and analytical
support for such a scaling law is strong. The unusual
correction term in Eq. (11) may arise from the non-self-
averaging properties of the critical clusters. A similar law,
but with $b < 0$, has been found for conformations of
random walks on percolation clusters [34].

In any case, our results clearly disprove that μ results as
the undiluted value [35] times the critical concentration
[36], $\mu \approx p_c \mu_{full} = 1.459\,583(3)$, claimed in [16,19,32].
By restricting the range of N, we again get a similar value,
which is probably due to finite-size effects: Initially, the
lattice defects and the self-avoidance act independently;
only with increasing N does their interplay and the top-
ology of the clusters become relevant. The asymptotic
behavior might, for instance, be affected by the distribution
of loop sizes on the cluster (backbone), or by the spatial
distribution of regions that contribute disproportionately to
the entropy, which cannot be gauged by short walks.

In summary, we have presented a method to exactly
enumerate SAWs of over 10^4 steps on three-dimensional
critical percolation clusters. This enabled a firm analysis of
the asymptotic scaling behavior of the end-to-end distance
with unprecedented accuracy. We revised the established
estimate for the leading scaling exponent, verified the
hypothesis $\nu_{ic} = \nu_{bb}$, and gave a first estimate for the
confluent correction exponent Δ.

Direct investigation of the average number of confor-
mations $[Z]$ was hampered by large deviations, rendering
our results less conclusive here. The nature of the distri-
bution of $\ln Z$, which resembles a Gaussian whose variance
we found to increase linearly with N, suggests that
information can be gleaned from the mean entropy,
$[\ln Z]$. Surprisingly, $[\ln Z]$ does not behave as expected,

which puts the commonly assumed scaling law for Z [Eq. (1)] into question as well.

Our findings show that the true asymptotic scaling behavior cannot be observed from system sizes accessible with other numerical tools. This observation may serve as a general lesson of caution regarding numerical studies of systems with strong (fractal) disorder, and calls for further applications of our new method. These may include other types of walks or media (or both). The SAW can be furnished with short-range interactions to model Θ-polymers [37,38], possibly under stretching force [17,39]. One can also add bending stiffness to study semi-flexible polymers [40,41]. The underlying idea of a scale-free partitioning is not even restricted to walk models but could be transferred to spin systems or transport processes. Of course, the necessary condition is that the medium has a weakly connected, self-similar geometry. One can obviously study percolation clusters of different dimensionality, even beyond the upper critical dimension of $D = 6$, to gain deeper understanding of the role of the medium's fractal dimensions. For $p > p_c$, the efficiency of our method eventually deteriorates, but it can still beat other methods near the critical concentration [23]. Further applications could include Ising and Potts clusters, diffusion limited aggregation (DLA) clusters, and possibly certain types of quantum gravity graphs [42] or real-world fractal networks [43].

[*]niklas.fricke@itp.uni-leipzig.de
[†]wolfhard.janke@itp.uni-leipzig.de

[1] N. Madras and G. Slade, *The Self-Avoiding Walk* (Birkhäuser, Boston, 1993).
[2] P.-G. de Gennes, *Scaling Concepts in Polymer Physics* (Cornell University Press, Ithaca, 1976).
[3] *Statistics of Linear Polymers in Disordered Media*, edited by B. K. Chakrabarti (Elsevier, Amsterdam, 2005).
[4] D. Ben-Avraham and S. Havlin, *Diffusion and Reactions in Fractals and Disordered Systems* (Cambridge University Press, Cambridge, 2000), Chap. 10.
[5] D. Stauffer and A. Aharony, *Introduction to Percolation Theory* (Taylor and Francis, London, 1992).
[6] Y. Meir and A. B. Harris, Phys. Rev. Lett. **63**, 2819 (1989).
[7] Y. Kim, J. Phys. C **16**, 1345 (1983).
[8] M. Sahimi, J. Phys. A **17**, L379 (1984).
[9] J. Hovi and A. Aharony, J. Stat. Phys. **86**, 1163 (1997).
[10] C. von Ferber, V. Blavatska, R. Folk, and Y. Holovatch, Phys. Rev. E **70**, 035104 (2004).
[11] H. K. Janssen and O. Stenull, Phys. Rev. E **75**, 020801 (2007).
[12] H. K. Janssen and O. Stenull, Phys. Rev. E **85**, 011123 (2012).
[13] H. Nakanishi and S. B. Lee, J. Phys. A **24**, 1355 (1991).
[14] C. Vanderzande and A. Komoda, Phys. Rev. A **45**, R5335 (1992).
[15] M. D. Rintoul, J. Moon, and H. Nakanishi, Phys. Rev. E **49**, 2790 (1994).
[16] A. Ordemann, M. Porto, H. E. Roman, S. Havlin, and A. Bunde, Phys. Rev. E **61**, 6858 (2000).
[17] A. R. Singh, D. Giri, and S. Kumar, Phys. Rev. E **79**, 051801 (2009).
[18] S. B. Lee and H. Nakanishi, Phys. Rev. Lett. **61**, 2022 (1988).
[19] K. Y. Woo and S. B. Lee, Phys. Rev. A **44**, 999 (1991).
[20] P. Grassberger, J. Phys. A **26**, 1023 (1993).
[21] V. Blavatska and W. Janke, Phys. Rev. Lett. **101**, 125701 (2008).
[22] V. Blavatska and W. Janke, Europhys. Lett. **82**, 66006 (2008).
[23] N. Fricke and W. Janke, Eur. Phys. J. Spec. Top. **216**, 175 (2013).
[24] N. Fricke and W. Janke, Europhys. Lett. **99**, 56005 (2012).
[25] A. Coniglio, N. Jan, I. Majid, and H. E. Stanley, Phys. Rev. B **35**, 3617 (1987).
[26] P. L. Leath, Phys. Rev. B **14**, 5046 (1976).
[27] N. A. Seaton and E. D. Glandt, J. Chem. Phys. **86**, 4668 (1987).
[28] M. E. J. Newman and R. M. Ziff, Phys. Rev. E **64**, 016706 (2001).
[29] R. Tarjan, Inf. Proc. Lett. **2**, 160 (1974).
[30] R. Rammal, G. Toulouse, and J. Vannimenus, J. Phys. (Paris) **45**, 389 (1984).
[31] A. Aharony and A. B. Harris, J. Stat. Phys. **54**, 1091 (1989).
[32] V. Blavatska and W. Janke, J. Phys. A **42**, 015001 (2009).
[33] N. Clisby, Phys. Rev. Lett. **104**, 055702 (2010).
[34] A. Giacometti and A. Maritan, Phys. Rev. E **49**, 227 (1994).
[35] R. D. Schram, G. T. Barkema, and R. H. Bisseling, J. Stat. Mech. (2011) P06019.
[36] X. Xu, J. Wang, J.-P. Lv, and Y. Deng, Front. Phys. **9**, 113 (2014).
[37] A. K. Roy and A. Blumen, J. Stat. Phys. **59**, 1581 (1990).
[38] K. Barat and B. K. Chakrabarti, Phys. Rep. **258**, 377 (1995).
[39] V. Blavatska and W. Janke, Phys. Rev. E **80**, 051805 (2009).
[40] A. Giacometti and A. Maritan, J. Phys. A **25**, 2753 (1992).
[41] D. Lekić and S. Elezović-Hadžić, Physica A **390**, 1941 (2011).
[42] W. Janke and D. A. Johnston, Nucl. Phys. **B578**, 681 (2000).
[43] C. Song, S. Havlin, and H. A. Makse, Nature (London) **433**, 392 (2005).